Biochemical Establishment and Characterization of EncM's Flavin-N5-oxide Cofactor

Robin Teufel,[†,#,◆] Frederick Stull,[‡,◆] Michael J. Meehan,[§] Quentin Michaudel,[⊥] Pieter C. Dorrestein,[§,†] Bruce Palfey,[‡,∥] and Bradley S. Moore*[,†,§]

[†]Center for Marine Biotechnology and Biomedicine, Scripps Institution of Oceanography, University of California, San Diego, California 92093, United States

[‡]Program in Chemical Biology, University of Michigan, Ann Arbor, Michigan 48109, United States

[§]Skaggs School of Pharmacy and Pharmaceutical Sciences, University of California San Diego, San Diego, California 92093, United States

[⊥]Department of Chemistry, The Scripps Research Institute, La Jolla, California 92037, United States

[∥]Department of Biological Chemistry, University of Michigan, Ann Arbor, Michigan 48109, United States

Ⓢ Supporting Information

ABSTRACT: The ubiquitous flavin-dependent monooxygenases commonly catalyze oxygenation reactions by means of a transient C4a–peroxyflavin. A recent study, however, suggested an unprecedented flavin-oxygenating species, proposed as the flavin-N5-oxide ($Fl_{N5[O]}$), as key to an oxidative Favorskii-type rearrangement in the biosynthesis of the bacterial polyketide antibiotic enterocin. This stable superoxidized flavin is covalently tethered to the enzyme EncM and converted into $FADH_2$ (Fl_{red}) during substrate turnover. Subsequent reaction of Fl_{red} with molecular oxygen restores the postulated $Fl_{N5[O]}$ via an unknown pathway. Here, we provide direct evidence for the $Fl_{N5[O]}$ species via isotope labeling, proteolytic digestion, and high-resolution tandem mass spectrometry of EncM. We propose that formation of this species occurs by hydrogen-transfer from Fl_{red} to molecular oxygen, allowing radical coupling of the formed protonated superoxide and anionic flavin semiquinone at N5, before elimination of water affords the $Fl_{N5[O]}$ cofactor. Further biochemical and spectroscopic investigations reveal important features of the $Fl_{N5[O]}$ species and the EncM catalytic mechanism. We speculate that flavin-N5-oxides may be intermediates or catalytically active species in other flavoproteins that form the anionic semiquinone and promote access of oxygen to N5.
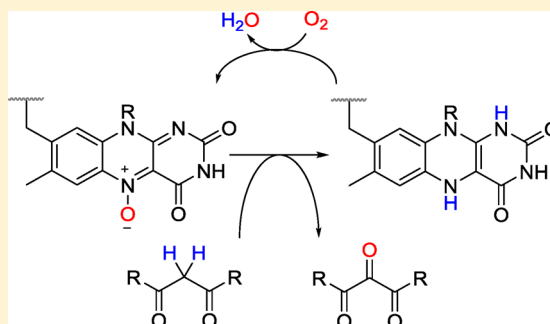
INTRODUCTION

The intensively studied flavoenzymes are found in all domains of life and carry out a variety of redox reactions such as the dehydrogenation or monooxygenation of organic substrates.[1−5] Except for a few unresolved cases,[6,7] oxygenation reactions are proposed to be exclusively mediated by transiently formed peroxy species bound to the C4a position of the flavin cofactor.[3,8−10] The formation of these reactive flavin-C4a–peroxides commonly requires the reduction of the flavin cofactor by the external electron donor NAD(P)H. Despite extensive studies over the last few decades, details of the subsequent reaction of O_2 with the reduced flavin (Fl_{red}) remain scarce. It is widely believed, however, that single-electron reduction of O_2 by Fl_{red} produces a superoxide anion and the neutral (blue) flavin semiquinone (SQ) radical with high spin density at C4a, which allows C4a–peroxide formation through radical coupling (see also Figure 3).[3,11] Surprisingly, in our recent work, ^{18}O-labeling studies and UV−vis spectroscopic analyses provided evidence for the presence of an unprecedented oxygenating species in the flavin adenine dinucleotide

(FAD)-dependent enzyme EncM,[12] which we proposed to be the flavin-N5-oxide (Figure 1). EncM catalyzes the key step in the biosynthesis of the unusual polyketide antibiotic enterocin (compound **1**, Figure 1) by *Streptomyces maritimus*.[12−16] The extremely reactive EncM substrate is synthesized by the type II polyketide synthase EncABC complex and the NADPH-dependent ketoreductase EncD, which convert benzoate and seven malonyl-CoA molecules to a C7-reduced acyl carrier protein (EncC)-bound poly(β-carbonyl) (**2**).[12−16] Remarkably, EncM alone proved sufficient for the following highly unusual oxidative Favorskii-type carbon−carbon rearrangement as well as aldol condensation and heterocycle forming reactions that give rise to desmethyl-5-deoxyenterocin.[16] Final pathway steps producing **1** are catalyzed by the hydroxylase EncR and methyltransferase EncK (Figure 1).[13,16] The flavin cofactor of EncM was found to be covalently tethered to a histidine residue (His78) within the active site, and the enzyme was shown to
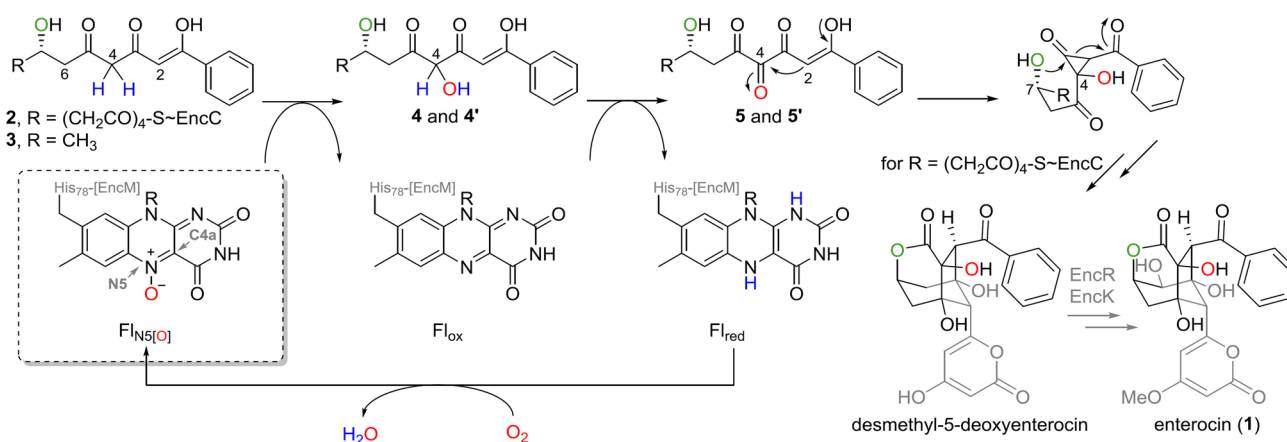
**Figure 1.** EncM-bound flavin-N5-oxide ($Fl_{N5[O]}$; dashed box, R = ribityl-ADP) mediates the dual oxidation of the natural polyketide substrate **2** (R = $(CH_2CO)_4$−S∼EncC) to **5** via **4** and the substrate analogue **3** (R = CH_3) to **5'** via **4'**. The oxidation triggers a Favorskii rearrangement that forms the lactone ring of **1**. EncM-bound $Fl_{N5[O]}$ becomes reduced in the process to Fl_{red}, which reacts with O_2 and regenerates $Fl_{N5[O]}$. For details of possible oxygenation mechanisms and $Fl_{N5[O]}$ formation, see ref 12 and Figure 3, respectively. EncM may also facilitate aldol condensation and heterocycle forming reactions to complete the formation of the tricyclic ring system and pyrone moiety of desmethyl-5-deoxyenterocin,[12,13,16] which is subsequently converted to **1** by EncR and EncK. Note that enzymatic formation of **2** by EncABCD is not shown.
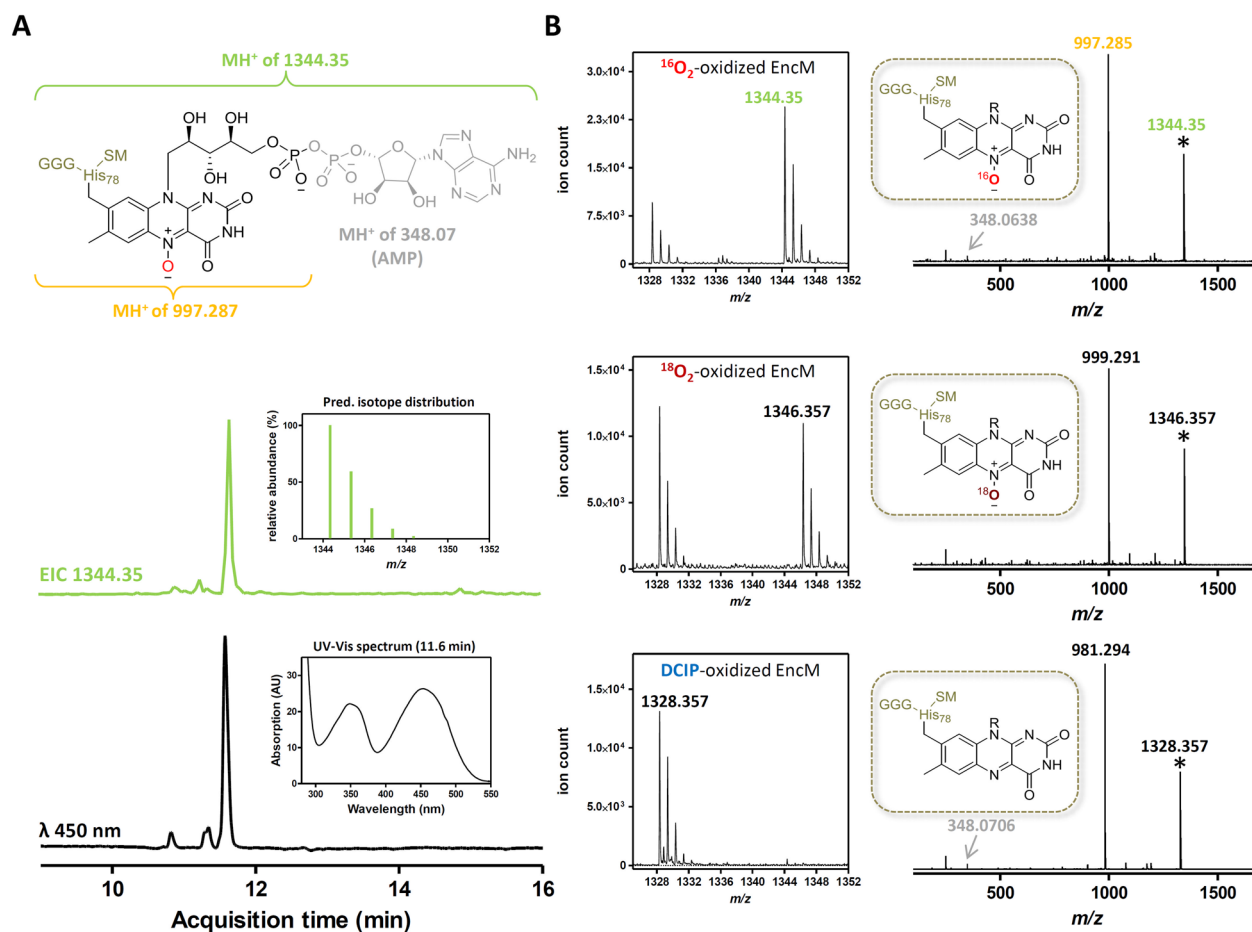
Figure 2. HR-ESI−LCMS data of proteinase K-digested EncM. (A) Top: Proposed structure of the detected flavinylated hexapeptide $GGGH_{78}[−Fl_{N5[O]}]SM$ with a calculated MH^+ of 1344.35. The fragments observed by MS^2 are indicated (see panel B). Middle: Extracted ion chromatogram (EIC) for the m/z of 1344.35 from the analysis of ($^{16}O_2$-oxidized) EncM and predicted isotope distribution for this molecule. Bottom: The chromatogram (λ 450 nm) and extracted UV−vis spectrum that confirm the simultaneous elution of the flavin cofactor at 11.6−11.7 min. (B) MS^1 (left side; narrowed m/z range showing the isotope distribution) and MS^2 spectra (right side; full m/z range, parent ions are indicated by the asterisks) recorded at 11.6 min of the flavinylated hexapeptide derived from $^{16}O_2$ (top), $^{18}O_2$ (middle), and DCIP-oxidized (bottom) EncM. Note that the $Fl_{N5[O]}$ species partially decayed to Fl_{ox} during EncM digestion and sample preparation, giving rise to some $GGGH_{78}[−Fl_{ox}]SM$ with a calculated MH^+ of 1328.355 (see also Supporting Information Figure S1). The respective oxidation states of the detected peptide-bound flavin cofactors are displayed within the dashed boxes (R = ribityl-ADP (parent ion) or ribosephosphate (fragment ions)).
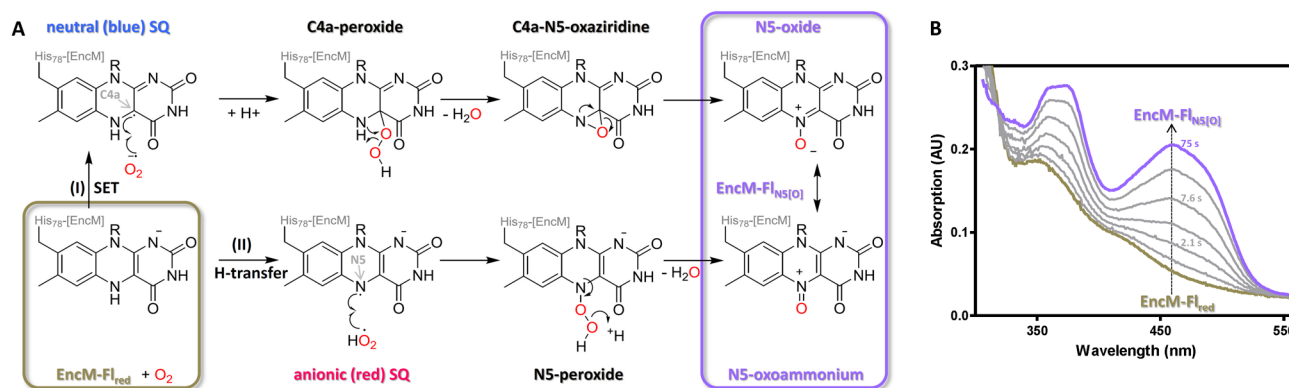
Figure 3. (A) Possible flavin-N5-oxide formation pathways (R = ribityl-ADP). Upper pathway (I): SET from EncM−Fl$_{red}$ (brown box) to O$_2$ may produce a superoxide anion and neutral (blue) semiquinone, allowing radical coupling at C4a. The C4a−peroxide may then rearrange to an oxaziridine upon elimination of water, which undergoes ring-opening to EncM−Fl$_{N5[O]}$. Lower pathway (II): On the basis of chemical reasoning and consistent with the data presented herein, the more likely route involves the direct Fl$_{N5[O]}$ formation at N5. Initial H-transfer from Fl$_{red}$ to O$_2$ yields anionic (red) SQ and protonated superoxide, which allows radical coupling at N5 before water elimination affords EncM−Fl$_{N5[O]}$. (B) Reaction of EncM−Fl$_{red}$ with O$_2$. Approximately 18 μM anaerobic EncM−Fl$_{red}$ was mixed with a final concentration of 615 μM O$_2$ in a stopped-flow spectrophotometer equipped with a diode-array detector. EncM−Fl$_{red}$ fully oxidized into EncM−Fl$_{N5[O]}$ without detectable intermediates over the course of 75 s.

trigger the Favorskii rearrangement through a hydroxylation/dehydrogenation dual oxidation (Figure 1).[12] Here, we set out to provide further experimental support for the proposed flavin-N5-oxide, gain insight into its enzymatic formation, and illuminate the catalytic mechanism of EncM in more detail using the synthetic substrate analogue 3 (Figure 1).[12]

■ RESULTS AND DISCUSSION

Spectroscopic Evidence for the Flavin-N5-oxide. The previously furnished biochemical evidence clearly established novel, oxidative flavin chemistry for EncM and suggested the involvement of a flavin-N5-oxide due to highly similar UV−vis spectra of chemically synthesized flavin-N5-oxide and the flavin cofactor bound to (native and denatured) EncM.[12] Yet, we did not provide direct support for the anticipated flavin-bound oxygen. Hence, we first aimed to acquire evidence for the proposed Fl$_{N5[O]}$ cofactor by mass spectrometry, as this species appeared stable within the EncM active site[12] in contrast to the transiently formed C4a−peroxide of common flavin-dependent monooxygenases.[3] For facile isolation and characterization of the cofactor, we attempted to disrupt the covalent link between the His$_{78}$ residue in heterologously produced EncM and the flavin cofactor by site-directed mutagenesis. However, replacement of His$_{78}$ with alanine, serine, or cysteine residues resulted in the formation of completely insoluble enzyme mutants and prevented further investigation. We thus digested native EncM with proteinase K, before separating and analyzing the peptide fragments via high resolution electrospray ionization liquid chromatography mass spectrometry (HR-ESI−LCMS, positive mode). This methodology allowed for the detection of small peptides[17] comprising His$_{78}$ bound to the Fl$_{N5[O]}$.

Concurrent with an absorption peak at 450 nm at 11.6 min indicating the flavin cofactor, we detected an ion with a m/z of 1344.35 that corresponded to the flavinylated hexapeptide GGGH$_{78}$[−Fl$_{N5[O]}$]SM (calculated (calcd) for C$_{47}$H$_{63}$N$_{17}$O$_{24}$SP$_2$: MH$^+$ of 1344.35) (Figure 2A). MS^2 data of this molecule provided further support for the presence of the flavin-N5-oxide by showing the characteristic loss of the adenosyl monophosphate moiety of FAD (−C$_{10}$H$_{14}$N$_5$O$_7$P), resulting in a m/z of 997.285 for the fragment ion (calcd for

C$_{37}$H$_{49}$N$_{12}$O$_{17}$SP: MH$^+$ of 997.287) (Figure 2B). Pseudo-MS^3 measurements further confirmed that the detected oxygen atom is indeed bound to the flavin cofactor rather than an amino acid residue (Supporting Information Figure S1). The same peptide fragment bound to conventional oxidized flavin was also detected (Figure 2B), arising from the partial decomposition of Fl$_{N5[O]}$ during proteolytic digestion and sample preparation, as confirmed by UV−vis spectroscopy (Supporting Information Figure S1).

Next, we sought to label the EncM-bound Fl$_{N5[O]}$ with ^{18}O to clearly link the observed mass to the presence of a flavin-bound oxygen atom. As previously reported,[12] dithionite reduces the postulated EncM-bound Fl$_{N5[O]}$ to Fl$_{red}$ under anaerobic conditions. Subsequent addition of molecular oxygen restores the Fl$_{N5[O]}$ species via an unknown pathway, whereas addition of the (nonoxygenic) oxidant dichlorophenolindophenol (DCIP) affords conventional, catalytically inactive oxidized flavin (Fl$_{ox}$).[12] Accordingly, we first reduced and then reoxidized EncM with either ^{18}O$_2$ or DCIP (as control), followed by proteinase K digestion and analysis of the peptide fragments as described above. As anticipated, a mass shift of 2 amu was detected for both the parent (m/z of 1346.357; calcd for C$_{47}$H$_{63}$N$_{17}$O$_{23}$SP$_2$[^{18}O]: MH$^+$ of 1346.354) and the fragment ions (m/z of 999.29; calcd for C$_{37}$H$_{49}$N$_{12}$O$_{16}$SP[^{18}O]: MH$^+$ of 999.291) of the flavinylated hexapeptide GGGHSM from ^{18}O$_2$-oxidized EncM. Importantly, DCIP-oxidized EncM exclusively showed conventional Fl$_{ox}$ with m/z of 1328.357 (calcd for C$_{47}$H$_{63}$N$_{17}$O$_{23}$SP$_2$: MH$^+$ of 1328.355) and 981.294 (calcd for C$_{37}$H$_{49}$N$_{12}$O$_{16}$SP: MH$^+$ of 981.292) for the respective molecules (Figure 2B). While mass spectrometry did not allow us to determine the percentage of EncM harboring the flavin-N5-oxide, previous spectroscopic comparison with chemically synthesized flavin-N5-oxide as well as the stoichiometry of ^{18}O-incorporation into the enzymatic product suggested that virtually all EncM-bound flavin is in the flavin-N5-oxide oxidation state.[12] Taken together, the hitherto reported biochemical and spectral evidence[12] and the MS data presented in this work provide compelling evidence for the novel flavin-N5-oxide oxygenating species of EncM.
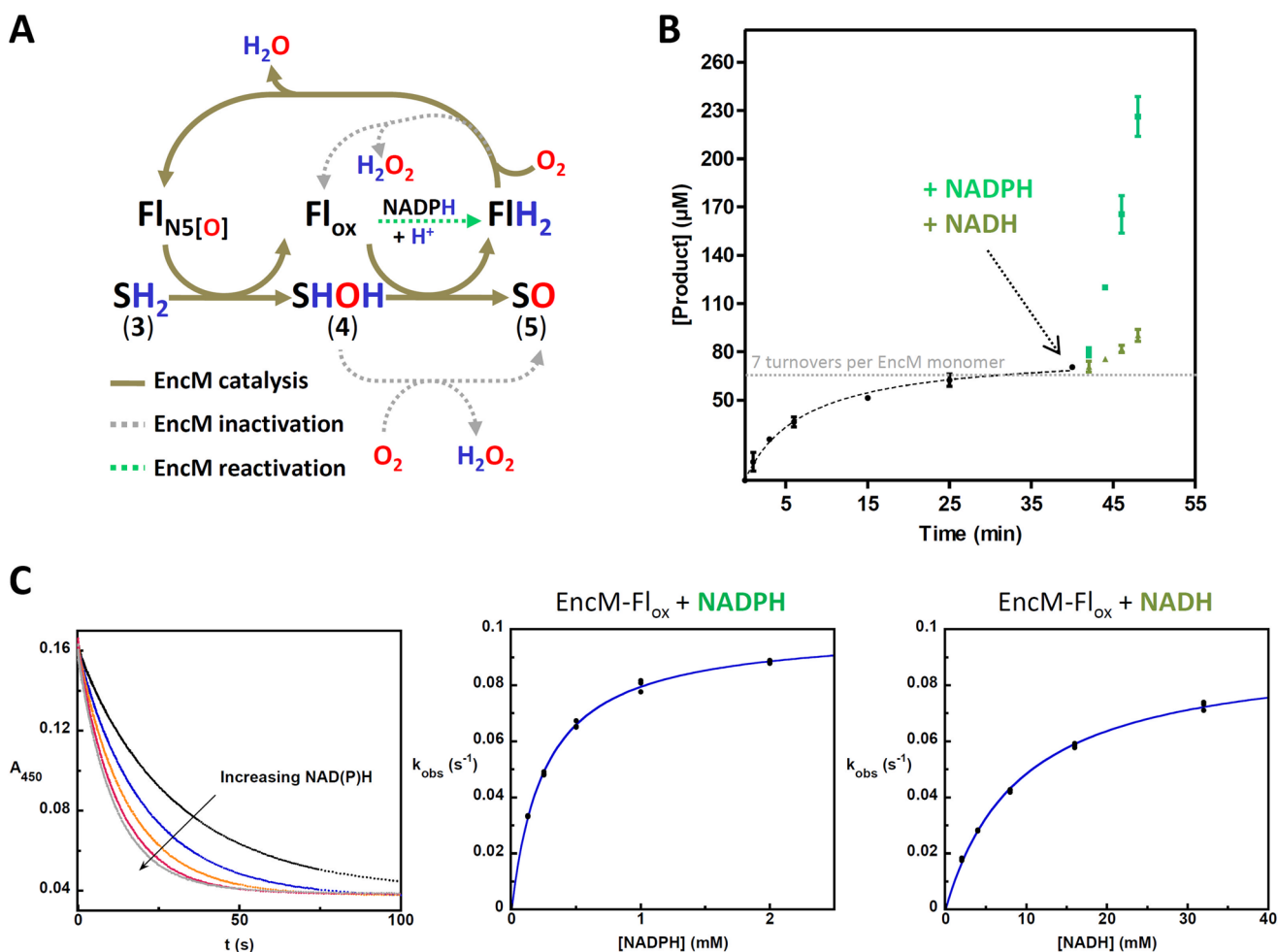
Figure 4. (A) Scheme of the EncM catalytic mechanism. Proposed catalytic steps and enzyme inactivation are shown with brown and gray arrows, respectively. NADPH can induce regeneration of EncM−$Fl_{N5[O]}$ once inactivation has occurred (green arrow). S = substrate (see Figure 1 for structures). (B) EncM (9.3 μM) catalyzed product formation. At least two independent samples were measured for each point of time. Error bars indicate the standard error. Due to EncM inactivation, each monomer formed an average total of ~7 product molecules. Splitting of the assay after 40 min of incubation and addition of either NADPH or NADH (1 mM each) restored the catalytic activity. (C) Stopped-flow analyses of the reaction of EncM−Fl_{ox} with NADPH and NADH. Left panel: Reaction traces for the reduction of EncM−Fl_{ox} by NAD(P)H. Approximately 14 μM EncM−Fl_{ox} was mixed anaerobically in a stopped-flow spectrophotometer with final concentrations of 0.125−2 mM NADPH or 2−32 mM NADH at 4 °C. Reduction of the flavin was monitored at 450 nm. All traces fit to a single exponential. The middle and right panel show the observed rate constants for flavin reduction as a function of the concentration of NADPH or NADH, respectively. The observed rate constant varied hyperbolically with either pyridine nucleotide, reaching a limiting value for the rate constant of flavin reduction (k_{red}) of 0.100 ± 0.001 s^{-1} for NADPH and 0.093 ± 0.001 s^{-1} for NADH. The apparent K_d values from the fits were 260 ± 10 μM and 9.3 ± 0.3 mM for NADPH and NADH, respectively.

Proposed Pathway for the Enzymatic formation of the Flavin-N5-oxide. EncM catalyzes the $Fl_{N5[O]}$-mediated oxidative transformation of the C4-methylene group of **2** (or **3**) to a ketone. This dual oxidation formally comprises the introduction of a hydroxyl group through monooxygenation producing **4** (or **4′**), followed by a dehydrogenation step that yields **5** (or **5′**) (Figure 1). In the process, the $Fl_{N5[O]}$ is completely reduced to Fl_{red}, which allows subsequent reaction with molecular oxygen and restoration of the $Fl_{N5[O]}$ via an unknown route.[12] One conceivable pathway for $Fl_{N5[O]}$ generation involves the transient formation of a flavin-C4a−peroxide via single electron transfer (SET) from Fl_{red} to O$_2$ and subsequent radical coupling at C4a, analogous to conventional flavin-dependent oxygenases.[3] The peroxide could then further rearrange to a ring-strained C4a−N5 oxaziridine that opens up to the $Fl_{N5[O]}$ (route I, Figure 3). This oxaziridine was debated more than 30 years ago as a possible intermediate in flavin-dependent oxygenases before the C4a-peroxide oxygenating

species was universally accepted.[18,19] Yet, the geometry of the flavin-C4a−peroxide strongly suggests that formation of the ring-strained oxaziridine is unlikely to occur, as the bond-forming N5 lone pair faces away from the proximal O of the peroxide (Supporting Information Figure S2). To date, this rearrangement has never been observed for any flavoprotein. We consequently consider oxaziridine formation improbable and instead propose a mechanism that involves the direct reaction of O$_2$ with N5 of the flavin. An initial net transfer of a hydrogen atom from the N5 of Fl_{red} to O$_2$ (in a one-step reaction or in two steps through SET directly followed by proton transfer) may thus produce flavin SQ and protonated superoxide, followed by radical coupling to yield a short-lived flavin-N5-peroxide. Subsequent water elimination would then give rise to the N5-oxoammonium resonance form of the $Fl_{N5[O]}$ (route II, Figure 3). Importantly, we observed that EncM in fact stabilizes the anionic (red) flavin SQ[12] (rather than the neutral SQ) upon single-electron reduction under

anaerobic conditions, a feature that has been observed for a significant number of flavoproteins. As the anionic SQ is known to have high spin density at N5,[20,21] it provides a rationale for why the attack of superoxide and radical coupling during $Fl_{N5[O}$ formation may preferentially occur at N5 of EncM's flavin cofactor rather than C4a (Figure 3A). Notably, in contrast to conventional SET from Fl_{red} to O_2 leading to the formation of neutral SQ, we invoke a hydrogen transfer that produces protonated superoxide and the anionic SQ as the first step en route to the $Fl_{N5[O]}$. This reaction still complies with quantum mechanical spin conservation and directly produces the anionic SQ without the requirement for a catalytic base to remove the proton from N5 of the flavin. Moreover, it circumvents the formation of two anions in van der Waals contact (i.e., the superoxide anion and the anionic SQ), which would then need to react.

Stopped-flow experiments are consistent with our proposal for $Fl_{N5[O]}$ formation, as O_2 oxidized EncM-Fl_{red} into EncM–$Fl_{N5[O]}$ without detectable formation of a C4a–peroxide or other intermediates (Figure 3B). Moreover, chemical precedence lends further credence for this route, as similar enamine autoxidations[22,23] are proposed to produce protonated superoxide through the net transfer of a hydrogen atom to O_2[22] and N-bound peroxides were previously reported too[24,25] (in the form of more stable N–O–O–t-Bu species). Formation of the anionic SQ may be promoted by hydrogen-bond donors from the protein to stabilize the negative charge in the N1–C2=O region.[20] The Tyr416 residue of EncM as well as the cofactor's 2′-hydroxyl group of the ribityl chain are in hydrogen bonding distance to O_2 (2.53 Å) and N1 (2.76 Å), respectively, and could thus fulfill that role (Supporting Information Figure S3). Replacement of Tyr416 with phenylalanine resulted again in an insoluble EncM mutant and prevented further investigation.

Substrate Reactivity May Impose Intricate Catalytic Requirements on EncM. One peculiarity of EncM's catalytic mechanism is the progressive enzyme inactivation during processing of substrate **3** (∼14% of enzyme becomes inactivated per turnover), resulting in an average total formation of ∼7 products per EncM monomer.[12] This inactivation is caused by incomplete regeneration of the $Fl_{N5[O]}$ species during the catalytic cycle that ultimately transforms all EncM-bound $Fl_{N5[O]}$ into Fl_{ox}.[12] One scenario for inactivation is the formation of a labile flavin-bound intermediate (e.g., the N5-peroxide; see Figure 3) that in rare cases eliminates H_2O_2 instead of water, thereby giving rise to Fl_{ox} instead of $Fl_{N5[O]}$. To test this hypothesis, we reoxidized EncM–Fl_{red} with O_2 to form EncM–$Fl_{N5[O]}$ and monitored the formation of H_2O_2. H_2O_2 was generated in ∼4% of the flavin reoxidation events, which, however, cannot fully account for the observed EncM inactivation rate (Supporting Information Figure S4). In addition, one can envisage inactivation through withdrawal of the reactive intermediate **4′** (e.g., through spontaneous cyclization or autoxidation), which would prevent the dehydrogenation step that affords Fl_{red} needed to regenerate $Fl_{N5[O]}$. As no shunt products accumulated in detectable amounts during EncM substrate turnover, we hypothesize that atmospheric O_2 spontaneously oxidizes **4′** to **5′** in a reaction that not only directly competes with the slow, rate-limiting flavin-mediated dehydrogenation step,[12] but also mimics its outcome (Figure 4A). The known propensity of α-hydroxy diketone compounds like **4′** for autoxidation[26] substantiates this scenario. A byproduct of this detrimental reaction would be H_2O_2, whose EncM-dependent formation

was indeed significantly increased during substrate turnover (Supporting Information Figure S4).

EncM inactivation raises interesting questions regarding the oxygen availability within the active site. On the one hand, O_2 is required to generate the flavin oxygenating species, while on the other hand, its access to the active site during substrate turnover would have to be controlled to avoid **4** autoxidation and formation of toxic H_2O_2. This predicament might provide a rationale for the confined EncM substrate binding tunnel[12] and the employment of a preformed oxygenating species. The sizable natural substrate **2** largely fills out the internal cavity of EncM, which may not only prevent spontaneous **2** cyclization but also displace oxygen to counteract autoxidation of intermediate **4**. After the final product is expelled from the active site, O_2 can react with Fl_{red} and restore $Fl_{N5[O]}$. Notably, our mechanistic studies with EncM had to be conducted with the significantly smaller substrate analogue **3** and the naturally occurring inactivation of EncM may therefore be less drastic with the full-length EncC-bound substrate **2**.

The Distinct Reactivity of EncM toward Reductants Suggests a Biological Role for NADPH. In contrast to most flavin oxygenases that employ external reductants for the formation of the oxygenating species, EncM uses its substrate as an electron donor and can thus be considered a rare member of the "internal monooxygenases".[4,12,27] However, due to occasional enzyme inactivation and EncM–Fl_{ox} formation, we surmised that exogenous reductants may allow substrate-independent flavin reduction and thus have an auxiliary role in the restoration of EncM-$Fl_{N5[O]}$. To investigate this proposal, we compared the EncM reaction in the presence and absence of the common natural reductants NADH and NADPH. Indeed, NADPH had a substantial effect on EncM catalysis and efficiently restored enzymatic activity in the presence of O_2 through restoration of EncM-$Fl_{N5[O]}$ (Figure 4B), as also verified by UV–vis spectroscopy (Supporting Information Figure S5). Reduction of EncM–Fl_{ox} by NADH, however, was significantly slower. Stopped-flow analyses indicated that this difference in reactivity is caused by a ∼36-fold lower binding affinity for NADH (apparent K_d of 9.3 mM) compared to NADPH (apparent K_d of 0.26 mM), whereas the rate constants for flavin reduction by NADH (0.093 s^{-1}) and NADPH (0.100 s^{-1}) were almost identical (Figure 4C). These results imply that EncM has evolved a selectivity for NADPH, despite the lack of a dedicated NAD(P)H binding site.[12] The EncM structure suggests that NADPH can only access the substrate binding tunnel and the active site in the absence of substrate **2**. To further investigate this, we crystallized EncM with 4 mM NADPH and determined the structure at a resolution of 1.7 Å. No significant conformational changes were observed compared to apo-EncM[12] and the disordered electron density within the active site regrettably did not allow elucidation of the NADPH binding mode (Supporting Information Figure S6).

Interestingly, although (chemically synthesized) flavin-N5-oxide was reported to be susceptible to reduction,[28] NAD(P)H reacted drastically slower with EncM–$Fl_{N5[O]}$ than with EncM–Fl_{ox} (Figure 4C and Supporting Information Figure S7). This selective reactivity likely prevents futile consumption of NAD(P)H *in vivo* and accounts for the stimulating effect of these reducing agents on EncM.

The Significance and Role of the Flavin-N5-oxide as a Biological Oxidative Agent. At present, EncM is the only reported enzyme that utilizes a flavin-N5-oxide. We openly question whether this is the rare exception or the proverbial tip

of the iceberg. One of the reasons why this species may have been overlooked in the past is the limited usefulness of protein crystallography for the detection of cofactor redox states, as X-ray radiation induces artifactual reduction of flavins and other redox centers.[29,30] Accordingly, the diffraction data for EncM did not support an N5-bound oxygen.[12] This could also apply to other structurally resolved enzymes that employ a flavin-N5-oxide. Similarly, dithiothreitol (DTT), which is frequently used for protein purification/storage,[31] reduced the flavin-N5-oxide in EncM (Supporting Information Figure S5) and, thus, impeded its detection by UV−vis spectroscopy, a key diagnostic tool for flavoproteins. Notably, the biological thiol-containing reductant glutathione, in contrast, did not affect EncM−Fl$_{N5[O]}$ (Supporting Information Figure S5). Finally, even intact flavin-N5-oxides can easily be mistaken for ordinary oxidized flavin due to their similar (but not identical) spectral features.[12]

Yet, it is plausible that other flavoproteins may generate the flavin-N5-oxide as well. The key structural features of EncM are similar to common flavoproteins with the vanillyl-alcohol oxidase/p-cresol methylhydroxylase (VAO/PCMH) fold and it employs no other cofactors (e.g., transition metals) that could participate in Fl$_{N5[O]}$ formation.[12,32] Moreover, EncM−Fl$_{N5[O]}$ generation readily occurs at ambient temperatures by the reaction of Fl$_{red}$ with O$_2$ (Figure 3B). We thus conclude that flavin-N5-oxide formation is thermodynamically accessible to simple flavoproteins and may require stabilization of the anionic SQ form and access of O$_2$ to N5. More flavin-N5-oxide employing enzymes are necessary to further define the chemical properties and reactivities of this newly recognized biological oxidant. Conceivably, it may allow versatile oxidative chemistry, as N-oxides are nucleophilic in nature, whereas its oxoammonium resonance form (Figure 3) is electrophilic, analogous to the anionic and protonated forms of the flavin-C4a−peroxide, respectively.[3] Fine tuning of the flavin cofactor through the surrounding amino acids may thus promote electrophilic or nucleophilic oxidation reactions. Moreover, N-oxyl radicals, such as the phthalimide-N-oxyl (PINO) radical, are widely used in organic chemistry as single-electron oxidants[33] and similar radical-type chemistry can be envisaged for flavin-N5-oxides. With the flavin-N5-oxide added to the repertoire of the flavin monooxygenases, it is interesting to compare flavin monooxygenases to iron monooxygenases such as cytochromes P450.[34−36] Both types of enzymes can oxygenate substrates using (hydro)peroxide intermediates, i.e., oxygenation of the substrate occurs before or with the cleavage of the O−O bond. However, they can also cleave the O−O bond en route to forming the oxygen-transferring species. The hypervalent iron-oxo intermediates of cytochromes P450 are extremely unstable and are well-suited for reacting with unactivated substrates like alkanes. In contrast, the flavin-N5-oxide is stable and represents the resting form of EncM obtained from enzyme purification, suggesting that the intermediate−or, more properly, the new flavin redox state−is a safely active oxygen form adapted for reactive substrates.

CONCLUDING REMARKS

After decades of intensive flavoprotein studies, the surprising discovery of a novel, catalytically relevant flavin oxidation state raises many interesting questions about its significance and role in nature. The unprecedented employment of the flavin-N5-oxide by the structurally inconspicuous EncM once more underscores that protein fold cannot predict flavoenzyme

function. In the future, the herein presented methodology can be used to reveal other flavoproteins that may employ this stable, superoxidized flavin cofactor. Ultimately, this might provide a comprehensive picture of the enzymatic formation, chemical potential, and prevalence of the flavin-N5-oxide.

EXPERIMENTAL SECTION

Gene Cloning, Heterologous Protein Expression, and Purification. Procedures for EncM were described before.[12] After Ni^{2+}-NTA column purification of EncM, we observed residual contamination with catalase in our H$_2$O$_2$ detection assays. Hence, before quantification of H$_2$O$_2$ formation, EncM was further purified by a HiLoad 26/60 Superdex 200 column equilibrated with buffer containing 20 mM HEPES-Na$^+$ (pH 7.5), 0.3 M NaCl, and 10% (v/v) glycerol, which removed contaminating catalase and afforded highly pure EncM.

Site-Directed Mutagenesis. The expression plasmid pHIS8-EncM (12) was used for site-directed mutagenesis with the QuikChange site-directed mutagenesis kit according to protocol (Stratagene, La Jolla, CA). The following oligonucleotide and respective complementary primer were used to obtain the EncM mutant M80I: Fw, 5′-GGCGGCGGACACAGCATTGCCGGGC-ACTCGGTATG-3′; Rv, 5′-CATACCGAGTGCCCGGCAAT-GCTGTGTCCGCCGCC-3′. The mutation was confirmed by sequence analysis.

Chemical Synthesis. The syntheses of substrate analogue **3** and the flavin-N5-oxide were described before.[12]

EncM (Re)oxidation with DCIP, ^{16}O$_2$ and ^{18}O$_2$. The procedure (Figure 2 and Supporting Information Figure S1) was conducted as described before.[12]

EncM Digestion and Analysis by Mass Spectrometry. (Figure 2 and Supporting Information Figure S1). Final concentrations of 2.5−3.8 mg/mL of native EncM (DCIP, ^{16}O$_2$, and ^{18}O$_2$-oxidized) or EncM-M80I were digested for 4−6 h at 22 °C in the dark with 2 mg/mL fungal proteinase K (Life Technologies TM, Carlsbad, CA) in 25 mM Tris-HCl (pH 7.8) supplemented with 5 mM CaCl$_2$. The digestion mixtures were then applied to Nanosep spin columns (Pall Corporation, Port Washington, NY) with a molecular weight cutoff of 10 kDa and centrifuged at 13 000g for 30 min. The yellowish flowthroughs containing the peptide fragments were subsequently analyzed by HR-ESI−LCMS (positive mode) with an m/z range of 100−1700 using a 1290 Infinity LC system coupled to a 6530 Accurate-Mass Q-TOF MS system (Agilent Technologies, Santa Clara, CA). LC was conducted with a Luna 5 μm C18E (2) column (Phenomenex, Torrence, CA) (150 × 4.6 mm) using a MeCN gradient of 2−100% (v/v) over 25 min in 0.1% (v/v) formic acid. MS2 spectra were acquired using collision-induced dissociation (CID) 35 with a fragmentor voltage of 175 V. For pseudo-MS3 measurements,[37] the in-source fragmentor voltage was increased to 430 V.

Crystallization, Structure Determination, and Refinement of EncM. (PDB 4XLO) These procedures were conducted as described before.[12] The reservoir solution was prepared without DTT. A final concentration of 4 mM NADPH was added to the protein solution prior to mixing with the reservoir solution.

Stopped-Flow Experiments. (Figures 4 and 3B). Figure 4: Stopped-flow experiments were performed using a Hi-Tech Scientific KinetAsyst SF-61 DX2 stopped-flow spectrophotometer at 4 °C in 0.1 M Tris-H$_2$SO$_4$, pH 7.5, 10% glycerol. Enzyme solutions were made anaerobic in glass tonometers by repeated cycles of vacuum and equilibration with anaerobic argon. For the reduction kinetics, ~14 μM EncM−Fl$_{ox}$ was mixed with final concentrations of 0.125−2 mM NADPH or 2−32 mM NADH. NAD(P)H solutions were made anaerobic by bubbling with anaerobic argon. Reaction traces were monitored at 450 nm and fit to a single exponential in KaleidaGraph. The observed rate constant for flavin reduction increased hyperbolically with NAD(P)H concentration. The rate constant for flavin reduction (k_{red}) and the apparent K_d for NADPH and NADH were determined by fitting the observed rate constant versus the NADPH or NADH concentration to a hyperbola in KaleidaGraph. Figure 3B: The

EncM-bound flavin was reduced anaerobically in the tonometer by titrating with sodium dithionite. Approximately 18 μM EncM–Fl$_{red}$ (after mixing) was mixed with buffer that had been bubbled at 25 °C with 100% O$_2$ (615 μM O$_2$ after mixing), and the reaction was monitored by diode-array.

Enzyme Assays. (Figure 4). Product formation was determined at 22 °C using two replicate assays containing 20 mM HEPES-Na$^+$ (pH 7.5), 300 mM NaCl, ≥10% (v/v) glycerol, 0.7 mM **3**, and 9.3 μM EncM. EncM concentrations were adjusted based on the molar extinction coefficient of EncM–Fl$_{N5[O]}$ (9600 M^{-1} cm^{-1}) at 460 nm.[12] Samples were sequentially withdrawn and quenched after 1, 3, 6, 15, 25, and 40 min. The assay was split and 1 mM of either NADPH or NADH was added. Further samples were obtained from both assays after additional 2, 4, 6, and 8 min of incubation time. The EncM products were subsequently analyzed and quantified by HPLC as described before.[12]

UV–Vis Spectrophotometry. (Supporting Information Figures S1 and S4). The flavin absorption spectra were analyzed using an Agilent Cary 50 UV–vis spectrophotometer or a Shimadzu UV-2501 PC.

H$_2$O$_2$ Measurements. (Supporting Information Figure S4). For quantification of the EncM-mediated formation of H$_2$O$_2$, the Pierce Quantitative Peroxide Assay Kit (Thermo Fisher Scientific, Waltham, MA) was used according to protocol. H$_2$O$_2$ production through EncM–Fl$_{red}$ oxidation: 8, 24, 40, and 56 μM EncM–Fl$_{ox}$ were incubated with 150 μM NADPH for 5 min under aerobic conditions (three replicates for each concentration). Each EncM-bound Fl$_{ox}$ underwent only a single reduction (to EncM–Fl$_{red}$) and reoxidation cycle (to EncM–Fl$_{N5[O]}$), as the formed EncM–Fl$_{N5[O]}$ reacts very slowly with NADPH (see Supporting Information Figure S7). Samples were quenched with the Pierce working reagent and incubated for 20 min at 22 °C. The produced H$_2$O$_2$ was quantified by UV–vis spectroscopy (absorption detection at 560 nm) with a H$_2$O$_2$ standard curve. H$_2$O$_2$ production during EncM substrate turnover: the reaction assay contained 8.7 μM EncM–Fl$_{N5[O]}$ with 0.2 mM **3** alone or additional 0.3 mM NADPH. Samples of two independent replicate assays were withdrawn and quenched after, 20, 40, 60, 120, 240, and 360 s, respectively. After incubation with working reagent for 20 min, the H$_2$O$_2$ concentration was quantified as described above.

Reaction of EncM with Dithiothreitol, Glutathione, and NADPH. (Supporting Information Figure S5). The UV–vis spectrum of EncM–Fl$_{N5[O]}$ (enzyme as isolated from *Escherichia coli*) was recorded, before addition of 2 mM DTT. Another spectrum was recorded after an incubation time of 15 min under aerobic conditions. The unreacted DTT was removed with a PD-10 column (GE Healthcare, Uppsala, Sweden) using 20 mM HEPES-Na$^+$ (pH 7.8), 300 mM NaCl, and 10% (v/v) glycerol as exchange buffer. An additional UV–vis spectrum was recorded after (re)concentration of EncM with a Vivaspin 6 (30 kDa exclusion size) column (GE Healthcare, Uppsala, Sweden). Lastly, 150 μM NADPH was added and the final spectrum recorded. To test the effect of glutathione, a fresh aliquot of EncM–Fl$_{N5[O]}$ was incubated for 15 min with 1 mM glutathione (instead of DTT) and the spectrum was recorded.

Reaction of EncM–Fl$_{N5[O]}$ with NADPH. (Supporting Information Figure S7). Fourteen micromolar EncM–Fl$_{N5[O]}$ was incubated with 0.5 mM NADPH under aerobic conditions in 20 mM HEPES-Na$^+$ pH 7.5 and 300 mM NaCl. The consumption of NADPH was monitored and quantified by UV–vis spectroscopy at a wavelength of 365 nm ($\varepsilon_{365\ nm}$ of 3500 M^{-1} cm^{-1} for NADPH).

ASSOCIATED CONTENT

Ⓢ Supporting Information

Contains Supporting Figures 1–7 showing additional data from MS, UV-vis spectroscopy, and X-ray crystallography experiments. The Supporting Information is available free of charge on the ACS Publications website at DOI: 10.1021/jacs.5b03983.

AUTHOR INFORMATION

Corresponding Author
*bsmoore@ucsd.edu

Present Address
#Center for Biological Systems Analysis (ZBSA), University of Freiburg, 79104 Freiburg, Germany.

Author Contributions
◆R.T. and S.F. contributed equally to the work.

Notes
The authors declare no competing financial interest.

REFERENCES

(1) Walsh, C. T.; Wencewicz, T. A. *Nat. Prod. Rep.* **2012**, *30*, 175−200.
(2) Chaiyen, P.; Fraaije, M. W.; Mattevi, A. *Trends Biochem. Sci.* **2012**, *37*, 373−380.
(3) Palfey, B. A.; McDonald, C. A. *Arch. Biochem. Biophys.* **2010**, *493*, 26−36.
(4) van Berkel, W. J.; Kamerbeek, N. M.; Fraaije, M. W. *J. Biotechnol.* **2006**, *124*, 670−689.
(5) Fraaije, M. W.; Mattevi, A. *Trends Biochem. Sci.* **2000**, *25*, 126−132.
(6) Baunach, M.; Ding, L.; Bruhn, T.; Bringmann, G.; Hertweck, C. *Angew. Chem., Int. Ed.* **2013**, *52*, 9040−9043.
(7) Smitherman, C.; Gadda, G. *Biochemistry* **2013**, *52*, 2694−2704.
(8) Massey, V. *J. Biol. Chem.* **1994**, *269*, 22459−22462.
(9) Entsch, B.; Ballou, D. P. *Biochim. Biophys. Acta* **1989**, *999*, 313−322.
(10) Entsch, B.; Ballou, D. P.; Massey, V. *J. Biol. Chem.* **1976**, *251*, 2550−2563.
(11) Pennati, A.; Gadda, G. *Biochemistry* **2011**, *50*, 1−3.
(12) Teufel, R.; Miyanaga, A.; Michaudel, Q.; Stull, F.; Louie, G.; Noel, J. P.; Baran, P. S.; Palfey, B.; Moore, B. S. *Nature* **2013**, *503*, 552−556.
(13) Cheng, Q.; Xiang, L.; Izumikawa, M.; Meluzzi, D.; Moore, B. S. *Nat. Chem. Biol.* **2007**, *3*, 557−558.
(14) Piel, J.; Hertweck, C.; Shipley, P. R.; Hunt, D. M.; Newman, M. S.; Moore, B. S. *Chem. Biol.* **2000**, *7*, 943−955.
(15) Hertweck, C.; Xiang, L.; Kalaitzis, J. A.; Cheng, Q.; Palzer, M.; Moore, B. S. *Chem. Biol.* **2004**, *11*, 461−468.
(16) Xiang, L.; Kalaitzis, J. A.; Moore, B. S. *Proc. Natl. Acad. Sci. U.S.A.* **2004**, *101*, 15609−15614.
(17) Sickmann, A.; Mreyen, M.; Meyer, H. E. *IUBMB Life* **2002**, *54*, 51−57.
(18) Rastetter, W. H.; Gadek, T. R.; Tane, J. P.; Frost, J. W. *J. Am. Chem. Soc.* **1979**, *101*, 2228−2231.
(19) Orf, H. W.; Dolphin, D. *Proc. Natl. Acad. Sci. U.S.A.* **1974**, *71*, 2646−2650.
(20) Massey, V.; Hemmerich, P. *Biochem. Soc. Trans.* **1980**, *8*, 246−257.
(21) Barquera, B.; Morgan, J. E.; Lukoyanov, D.; Scholes, C. P.; Gennis, R. B.; Nilges, M. J. *J. Am. Chem. Soc.* **2003**, *125*, 265−275.
(22) Angelova, V. T.; Vassilev, N. G.; Chauvin, A. S.; Koedjikov, A. H.; Ivanov, P. M.; Pojarlieff, I. G. *ARKIVOC* **2008**, *11*, 11−23.
(23) Kirmse, W.; Siegfried, R. *J. Am. Chem. Soc.* **1968**, *90*, 6565−6566.

(24) Wei, Y.; Ding, H. Q.; Lin, S. X.; Liang, F. S. *Org. Lett.* **2011**, *13*, 1674−1677.

(25) Forster, S.; Rieker, A.; Maruyama, K.; Murata, K.; Nishinaga, A. *J. Org. Chem.* **1996**, *61*, 3320−3326.

(26) Verhe, R.; Debuyck, L.; Dekimpe, N.; Derooze, A.; Schamp. N. *Bull. Soc. Chim. Belg.* **1978**, *87*, 143−152.

(27) Huijbers, M. M.; Montersino, S.; Westphal, A. H.; Tischler, D.; van Berkel, W. J. *Arch. Biochem. Biophys.* **2014**, *544*, 2−17.

(28) Walsh, C.; Fisher, J.; Spencer, R.; Graham, D. W.; Ashton, W. T.; Brown, J. E.; Brown, R. D.; Rogers, E. F. *Biochemistry.* **1978**, *17*, 1942−1951.

(29) Garman, E. F.; Nave, C. *J. Synchrotron Radiat.* **2009**, *16*, 129−132.

(30) Garman, E. F.; Owen, R. L. *Acta Crystallogr., Sect. D* **2006**, *62*, 32−47.

(31) Getz, E. B.; Xiao, M.; Chakrabarty, T.; Cooke, R.; Selvin, P. R. *Anal. Biochem.* **1999**, *273*, 73−80.

(32) Koetter, J. W.; Schulz, G. E. *J. Mol. Biol.* **2005**, *352*, 418−428.

(33) Coseri, S. *Catal. Rev.* **2009**, *51*, 218−292.

(34) Hrycay, E. G.; Bandiera, S. M. *Arch. Biochem. Biophys.* **2012**, *522*, 71−89.

(35) Podust, L. M.; Sherman, D. H. *Nat. Prod. Rep.* **2012**, *29*, 1251−1266.

(36) Ortiz de Montellano, P. R. *Chem. Rev.* **2010**, *110*, 932−948.

(37) Ginter, J. M.; Zhou, F.; Johnston, M. V. *J. Am. Soc. Mass Spectrom.* **2004**, *15*, 1478−1486.